Aerodynamic efficiency enhancement for asymmetric profiles

Viorel Bostan, *Marin* Guţu,* and *Valeriu* Odainâi

Technical University of Moldova, Department of Basics of Machinery Projecting, 9/8 Studentilor str., block of study nr. 6, Chisinau, Republic of Moldova

Abstract. This paper presents a solution for enhancement of aerodynamic efficiency for asymmetric airfoils. In order to increase the lift and reduce the drag forces for a blade segment, a groove was created on its surface. There were carried out experiments consisting in the analysis of two asymmetric airfoil segments of the same type in the wind tunnel. One segment was designed with the groove and the other without it. The optimum location of the groove was determined by means of CFD analysis. Simulation results were compared to test results and the CFD analysis model was validated.

1 Introduction

Utilization of wind potential at small scale is hampered by reduced efficiency of low-power wind turbines. In this regard, more research has been carried out over the last decades. Proposed solutions to increase the performance of wind turbines are based on optimization of blade geometry, the use of special elements to increase aerodynamic effects, the use of composite materials based on carbon fiber etc. One method to increase the aerodynamic efficiency of the wind turbine rotors is to provide the blades with suction ports. This solution is presented in the work of one of the co-authors of this article [1]. Another interesting study on the control of the suction flow of a rectangular wing is presented in the paper [2].

Based on these studies, our team has done some research on increasing the aerodynamic efficiency of blades for low power wind turbines (1-10 kW). A wind turbine blade segment was analyzed with asymmetrical aerodynamic profile that was equipped with a groove on the surface. There were carried out experiments consisting of measurement of the lift and drag forces of the blade section in the wind tunnel for different angles of attack. In order to measure lift and drag forces for the grooveless blade section the adhesive tape was used to cover it.

In order to determine the optimum location of the groove on the airfoil section several CFD analyses were performed using ANSYS software. The blade section model was obtained via additive manufacturing technology using the 3D printer. The stages of the researches are presented further in more detail.

* Corresponding author: maringutu8@gmail.com

2 Wind turbine blade segment analisys

2.1 Finite element analysis setup

2.1.1 Fluid domain modeling and meshing

Wind turbine blade segment and domain was designed in SolidWorks and then imported into the ANSYS Workbench software. The dimensions of the blade segment were chosen taking into account the dimensions of the available wind tunnel measuring section (100 mm span and 100 mm chord). The size of the groove opening was accepted by 2.5% of the chord length as recommended in the paper [2]. Several CFD analyzes were performed in order to determine the optimum distance x from the leading edge to the center of the channel. Figure 1 shows the parameters of the simulated blade segment with airfoil NACA 4412.

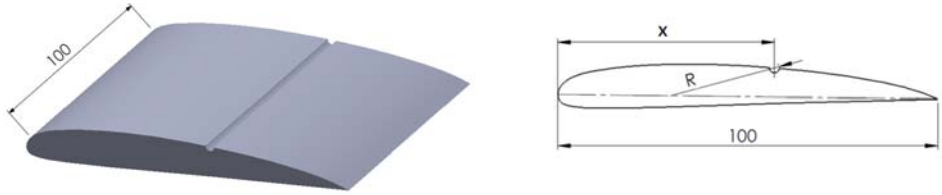

Fig. 1. Parameters of the simulated blade segment.

The dimensions of the computational fluid domain were chosen taking into account good practices and recommendations [3] so as to ensure free flow without influencing the boundaries of the field. Figure 2 *a* shows considered fluid domain. Mesh was generated in the ANSYS Meshing Workbench integrated program. After importing the geometric model the following regions required for computing were defined: (Inlet), (Outlet), (Walls). The basic dimensions of the mesh are specified by means of the minimum dimension Minimal size = 0.22 mm and Maximum Max Size = 30 mm of the faces of the elements and the adjacent volumes. The surface of blade segment was meshed as *Mapped Face* with the mesh size 0.5 mm (Figure 2, *b*). The transition from the fine-meshed areas to the gross meshed was done by specifying the Growth Rate = 1.1 expansion factor and the maximum variation in the characteristic dimensions of two adjacent elements is at most 5%. The entire domain was meshed into approx. 1859600 finite elements.

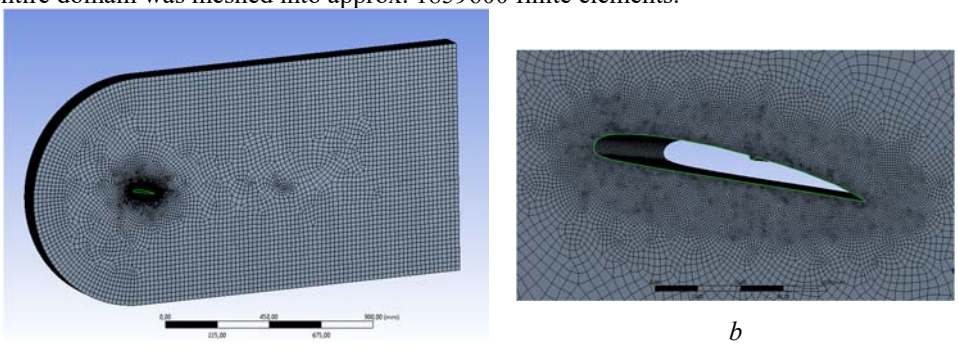

a *b*

Fig. 2. Meshed fluid domain (a) and details of boundary layer around the blade (b).

2.1.2 Boundary conditions setup

The boundary conditions imposed are the following: entry into the computing field is made by the boundary determined by the circular base of the upstream. At this border were imposed *Inlet* boundary conditions with the specification of the uniform and constant velocity distribution in the fixed reference system (V_0, 0, 0), where V_0 is wind speed. Outlet from the computing domain is made by the downstream border by specifying the *Outlet* boundary conditions with the average static pressure = 0. The top and bottom sides of the domain were subjected to *Walls* boundary conditions with the free-slip specification that simulates a zero-adhesion virtual wall. For the side walls that are in the same plane as the blade segment ends the *symmetry* boundary conditions have been set in order to exclude the influence of the turbulence at the edges. The surfaces of the blade segment was subject to *Walls* boundary conditions with "*no slip*" specification which does not allow mass or energy transfer, and the speed on these surfaces is considered equal to 0 in relation to the speed of the adjacent cells.

Velocity of airflow was considered 20 m/s which is close to the relative speed in the blade section at 1/2 of the rotor radius and is equivalent to Reynolds number of 150,000 for the 100 mm blade chord. The angle of attack of the blade segment was chosen 8 degrees for which the Lift/Drag ratio is maximum.

2.1.3 Solution and CFD results

For a better understanding of the results the velocity contour and turbulence kinetic energy around the blade segment section was analyzed, Figure 3 and 4. From Figure 3, *b* we can see the delay effect of separating the boundary layer on the surface of the blade section with groove.

In order to detect the influence of geometrical factors on blade's performance, turbulence kinetic energy is one of the indicators that helps identifying the regions of major turbulence that cause important energy flow losses. Physically turbulence kinetic energy is produced due to the mean flow gradients, and is dissipated by viscous effects [4].

For smooth surface blade section the maximum velocity is 29 m/s and turbulence kinetic energy is 10.5 J/kg. For blade section with groove the maximum velocity is 31.5 m/s and turbulence kinetic energy is 8 J/kg.

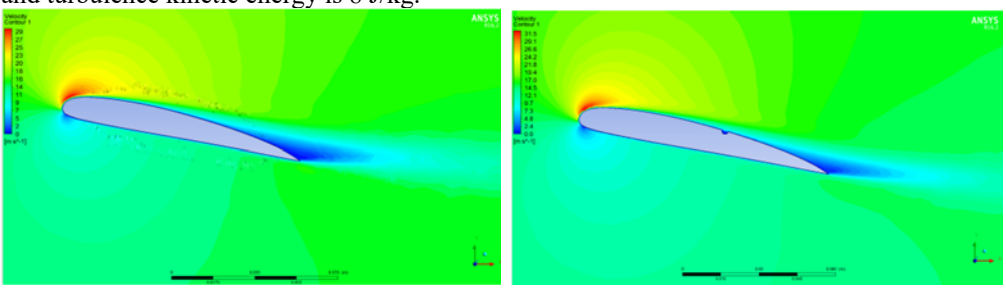

a *b*

Fig. 3. Velocity contour: *a* - smooth surface blade section; *b* - blade section with groove.

The value of the lift force of the blade segment fitted with groove was obtained approximately 6% lower than for the smooth blade segment. And drag force is decreasing with about 18% for blade segment fitted with groove.

The verification of these results is presented in the following paragraph by performing the tests in the wind tunnel.

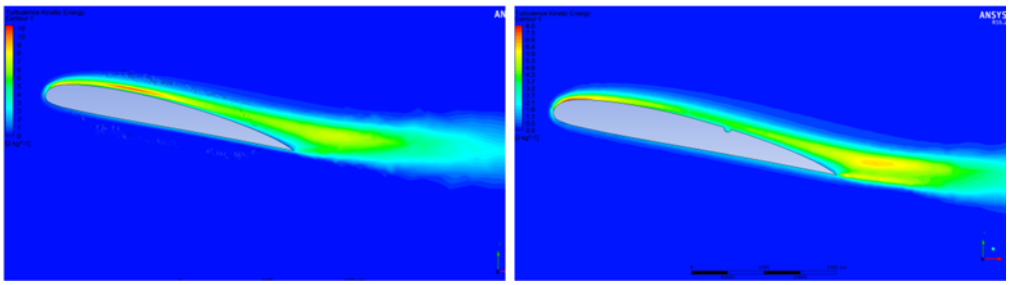

a *b*

Fig. 4. Turbulence kinetic energy: *a* - smooth surface blade section; *b* - blade section with groove.

2.2 Experimental setup

The experiment on the blade section consists in determining the lift and drag forces using educational wind tunnel [5], Figure 5.

Fig. 5. Educational wind tunnel.

The flow forces at the blade section are measured by an electronic two-component force measuring device. This device consists of a force transducer and a measurement amplifier with display.

The forces lift and drag are converted by means of the lever arm a of the model holder into proportional moments M, which deform a bending and torsion beam (Figure 6). The deformation is measured with a strain gauge and displayed digitally on the two-channel amplifier as force.

The blade section model was obtained via additive manufacturing technology using the 3D printer. In order to reduce the influence of the turbulence the blade segment was provided with plates at the ends, Figure 7 a. The blade segment mounted in the wind tunnel is shown in Figure 7 b.

The blade section was tested at the air velocity of 20 m/s for different angles of attack and the values of the lift and drag forces were recorded.

3 Results and discussions

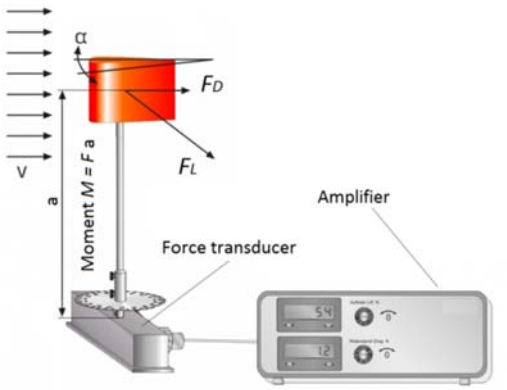

Fig. 6. Model holder and forces generation model.

Based on the analysis of the recorded results, the diagram of lift/drag ratio dependence on angle of attack was constructed, Figure 8. Also, the dependency diagram between lift force and angle of attack was drawn, Figure 9. The increase of the lift force for the grooved blade segment is by ≈5%. As can be seen from Figures 3 and 4, the main cause of the increase of the lift force and reduction of drag force consists in diminishing the negative influence of the separation of the fluid boundary layer on the upper surface of the blade section. Drag force values remained roughly the same.

a *b*

Fig. 7. Experimental setup: *a* - blade segment model, *b* - blade segment mounted in the wind tunnel.

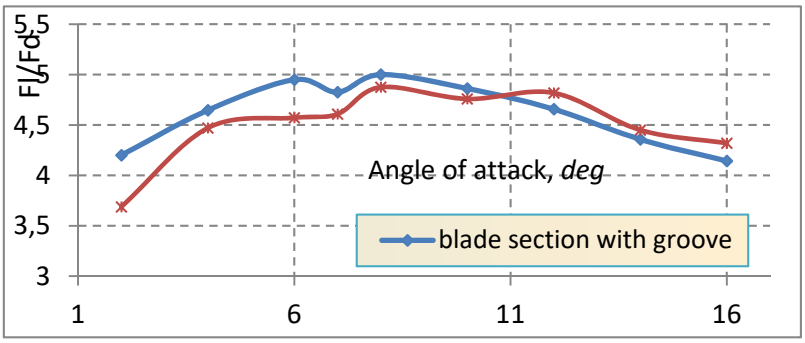

Fig. 8. Experimental results of lift/drag ratio dependence on angle of attack.

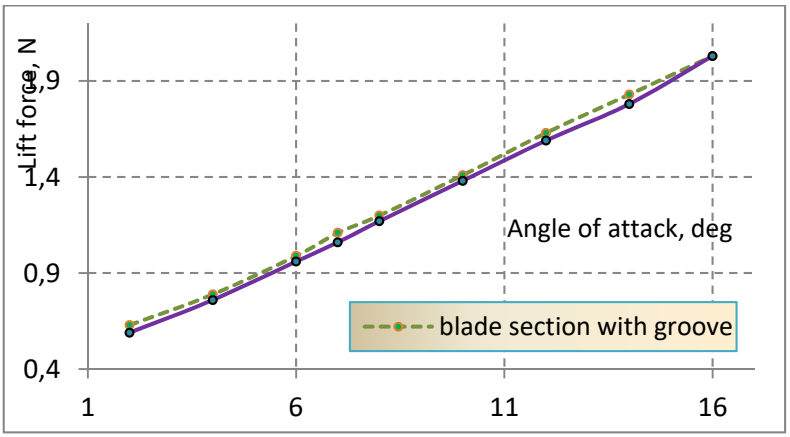

Fig. 9. Experimental results: the dependence between of lift force and angle of attack.

References

1. V. Bostan Wind turbine. Patent nr. 661 Y. Publication date 2013.07.31, BOPI no. 7/2013. 11 p
2. K. Yousefi, R. Saleh Three-dimensional suction flow control and suction jet length optimization of NACA 0012 wing, Springer Meccanica (2015)
3. V. Bostan Mathematical models in engineering. Contact issues. Modeling and simulations in aerodynamics. Chișinău: „Bons Office", 456, (2014)
4. Introduction to ANSYS FLUENT. Release 13.0, ANSYS Inc. 2013. 59, http://imechanica.org/files/fluent_13.0_lecture06-turbulence.pdf
5. http://gunt.de/index.php?option=com_gunt&task=gunt.list.category&lang=en&category_id=673